Vol 16 No 7, July 2007
1009-1963/2007/16(07)/2131-05

Chinese Physics

© 2007 Chin. Phys. Soc.
and IOP Publishing Ltd

Oxygen-vacancy-related dielectric relaxation and conduction mechanisms in $Bi_5TiNbWO_{15}$ ceramics*

Wang Xiao-Juan(王晓娟)[a], Gong Zhi-Qiang(龚志强)[a],
Qian Ya-Feng(钱亚峰)[a], Zhu Jun(朱 骏)[a], and Chen Xiao-Bing(陈小兵)[a,b]†

[a] *College of Physics Science and Technology, Yangzhou University, Yangzhou 225002, China*
[b] *The National Laboratory of Solid State Microstructure, Nanjing University, Nanjing* 210008*, China*

(Received 16 November 2006; revised manuscript received 14 December 2006)

This paper reports that the intergrowth ceramics $Bi_5TiNbWO_{15}$ (BW-BTN) have been prepared with the conventional solid-state reaction method. The dielectric and conductivity properties of samples were studied by using the dielectric relaxation and AC impedance spectroscopy in detail. Two distinct relaxation mechanisms were detected both in the plots of dielectric loss ($\tan\delta$) and the imaginary part (Z'') versus frequency in the frequency range of 10 Hz–13 MHz. We attribute the higher frequency relaxation process to the hopping process of the oxygen vacancies inside the grains, while the other seems to be associated with the space charges bound at the grain boundary layers. The AC impedance spectroscopy indicates that the conductivities at 625 K for bulk and grain boundary are about 1.12×10^{-2} S/m and 1.43×10^{-3} S/m respectively. The accumulation of the space charges in the grain boundary layers induces a space charge potential of 0.52 eV.

Keywords: intergrowth, dielectric relaxation, impedance spectroscopy, oxygen vacancies
PACC: 7740, 7280

1. Introduction

The intergrowth bismuth layer-structure ferroelectrics (IBLSFs), discovered first by Kikuchi *et al*,[1,2] have recently received considerable attention due to their relatively complex crystal structures and improved properties.[3–8] $Bi_5TiNbWO_{15}$, one kind of this intergrowth structure, is composed of one-half the unit cell of Bi_2WO_6 (BW, $m = 1$) and Bi_3TiNbO_9 (BTN, $m = 2$), with their perovskite blocks in turn sandwiched between $(Bi_2O_2)^{2+}$ layers. This material with a high ionic conductivity has great potential in the application of fuel cells, oxygen sensor, oxygen pumps, and chemical sensors, etc. These devices have the potential to deliver high economic and ecological benefits.

It is well known that the interior defects such as A-site vacancies, space charge electrons or oxygen vacancies have great influence on ferroelectric fatigue or ionic conductivity of the material.[9–12] Considering that the solid defects play a decisive role in all of these applications, we find that it is very important to gain a fundamental understanding of their conductive mechanism. Various kinds of defects are always suggested as being responsible for the dielectric relaxations at high temperature range. The AC impedance analysis is a powerful means to separate out the grain boundary and grain-electrode effects, which usually are the sites of trap for defects. It is also useful in establishing its relaxation mechanism by appropriately assigning different values of resistance and capacitance to the grain and grain boundary effects. In this paper, a detailed analysis of dielectric relaxation and AC impedance spectroscopy have been carried out to characterize the dielectric and conductivity properties of $Bi_5TiNbWO_{15}$ in order to gain insight into the relaxation mechanism and defects relation.

2. Experiment

The $Bi_5TiNbWO_{15}$ (BW-BTN) bulk samples were prepared with the conventional solid-state reaction method. Appropriate amounts of raw materials (in which excess Bi_2O_3 of 5.0 wt% of the stoichiometric composition was added to compensate for the volatilization of bismuth oxide during sintering at high temperatures) were first mixed by ball-milling

*Project supported by the National Natural Science Foundation of China (Grant No 10274066) and the Natural Science Foundation of Jiangsu Province, China (Grant No BK2005052).
†Corresponding author. E-mail: xbchen@yzu.edu.cn

for 24 h. After drying, the mixed powders were calcined at 800 °C for 8 h, then pressed into disc-shaped samples with a diameter of 12 mm and a thickness of about 1 mm. The samples were finally sintered at 980 °C in air for 4 h followed with the furnace cooling. To confirm the compound formation, the crystalline structure was characterized by the x-ray diffraction (XRD) method using an M03XHF$_{22}$ diffractometry (Cu K$\alpha, \lambda = 1.54056$ Å). The XRD patterns of the samples can fully indexed on the lattice cell reported in Ref.[2]. Dielectric and impedance measurements were carried out by using a low-frequency impedance analyser (HP-4192A) in air within the frequency range of 10 Hz–13 MHz.

3. Results and discussion

3.1. The measurement of dielectric relaxation versus frequency

Figure 1 shows the variation of dielectric loss (tanδ) with frequency at various temperatures. It is obvious that two peaks are superimposed on an apparent background increasing with the measuring temperature but decreasing with frequency. The higher-frequency peaks (denoted as $P_{\rm d1}$) are not obvious as the lower-frequency ones (denoted as $P_{\rm d2}$), but they do exist and are demonstrated clearly in Fig.1(b). The

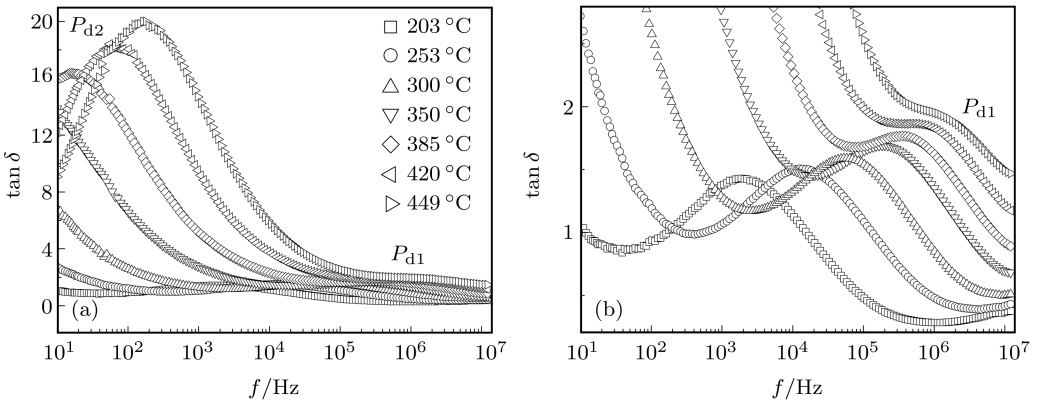


Fig.1. (a) The curves of dielectric loss versus frequency for $Bi_5TiNbWO_{15}$ sample at various temperatures. (b) $P_{\rm d1}$ loss peak versus frequency at a lower temperature range for clarity.

positions of both peaks apparently shift toward higher frequency with the increase of the peak height when temperature increases. This characteristic indicates that these two peaks are associated with a thermally activated relaxation process.

The relaxation essences of two dielectric peaks ($P_{\rm d1}$ and $P_{\rm d2}$) are further confirmed by the fact that similar phenomena are also observed in the plot of the imaginary part of Z'' versus frequency at various temperatures. There are also two peaks, marked with $P_{\rm Z1}$(higher-frequency range) and $P_{\rm Z2}$ (lower-frequency range) in the measuring frequency range as illustrated in Fig.2. The $P_{\rm Z2}$ peak is a typical Debye-like peak, whose peak position shifts towards higher-frequency and height decreases with the increase of the measuring temperature. But the $P_{\rm Z1}$ peak emerges at higher-frequency range is not obvious. It becomes very weak and shifts out of the frequency range when the temperature increases. A Debye-like peak in the frequency dependence of the imaginary part of impedance Z'' usually indicates the presence of space charges. The peak value of Z'' is proportional to the value of

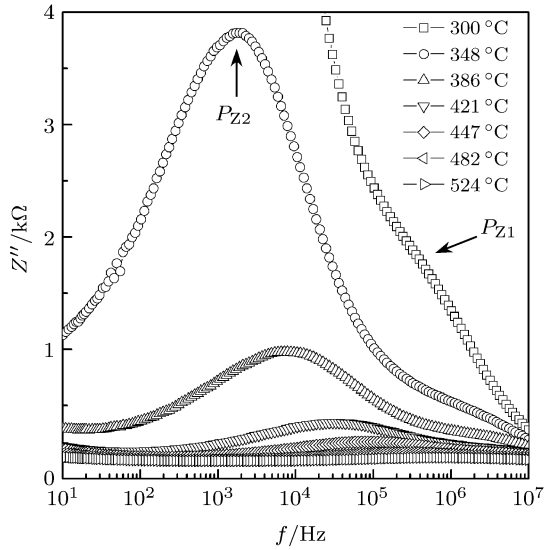


Fig.2. Frequency dependence of the imaginary part of impedance (Z'') measured at different temperatures for $Bi_5TiNbWO_{15}$.

R.[13−15] At lower frequency, the space charges may easily be bound up by the grain boundary, leading to a pronounced relaxation progress. With the increasing of the frequency, the space charge polarization is reduced. It becomes easier for them to relax and recombine with the vacancies in grain interiors.

For a thermally activated relaxation process, the relaxation time τ generally follows the Arrhenius law:

$$\tau = \tau_0 \exp(E_{\text{relax}}/k_B T), \tag{1}$$

where τ_0 is the pre-exponential factor (or the relaxation time at infinite temperature), T is the absolute temperature, E_{relax} denotes the activation energy of the relaxation process, and k_{B} is the Boltzmann constant. It is well known that at the peak position the condition $\omega_{\text{p}}\tau_{\text{p}} = 1$ is fulfilled, where $\omega = 2\pi f$ is the angular frequency of measurement and the subscript p denotes values at peak position. Therefore the relaxation parameters E_{relax} and τ_0 can be determined from the frequency spectra at different temperatures. If we plot $\ln(\omega_{\text{p}})$ as a function of the reciprocal of peak temperature, a linear relation would be obtained according to Eq.(1). The so-called Arrhenius plot for frequency dependence of the dielectric loss and the imaginary part of impedance are shown in Figs.3(a)

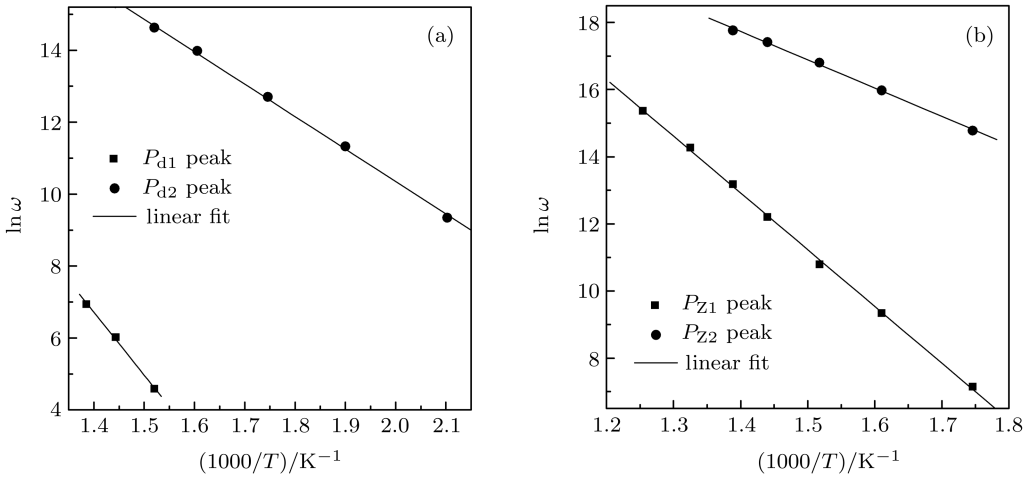


Fig.3. The Arrhenius plot of two relaxation peaks (a) dielectric loss peaks (P_{d1} and P_{d2}) and (b) imaginary part of impedance (P_{Z1} and P_{Z2}) from the frequency spectra.

and 3(b). Table 1 shows the results of such calculations for P_{d1}, P_{d2}, P_{Z1} and P_{Z2} peaks respectively. The relaxation parameters of higher-frequency peaks (P_{d1} and P_{Z1}) are very close to each other. As for the lower-frequency peaks (P_{d2} and P_{Z2}), the consistency is also well detected. This character indicates that the peaks of tanδ and Z'' appearing at the corresponding frequency range are attributed to the same relaxation mechanisms. Wang *et al* reported activation energy related to oxygen vacancy in $SrBi_2Ta_2O_9$was 0.97 eV,[16] Shulman *et al* have also shown that activation energy due to oxygen-ion jump in $Bi_4Ti_3O_{12}$ was 0.87 eV,[17] and Ang *et al* reported that the activated energy attributed to the motion of defects associated with ($V''_{\text{Sr}} - V_{\text{o}}^{\bullet\bullet}$) was 0.74–0.86 eV.[12] In comparison with above reports, the fitted results seem quite reasonable. Considering the analysis above, we should like to attribute the lower-frequency peak to the relaxation of the space charges associated with the oxygen vacancies at the grain boundary layer, and the higher-frequency peak to the oxygen vacancies relaxation inside the grains.

Table 1. The activation parameters for P_{d1}, P_{d2}, P_{Z1} and P_{Z2} peaks.

	P_{d1} peak	P_{d2} peak	P_{Z1} peak	P_{Z2} peak
E_{relax}/eV	1.50	0.78	1.46	0.73
τ_0/s	2.38×10^{-14}	4.69×10^{-13}	1.29×10^{-14}	1.50×10^{-13}

3.2. The measurement of complex impedance spectroscopy

Space charges are generally created due to the disparity in defect concentration and the inhomogeneity of the applied field. Thus the space charges existing in the samples may well be trapped in the grain boundary and grain–electrode interfaces. Complex impedance spectroscopy is a useful means capable of separating dielectric contributions of grain interior from that of grain boundary by modelling the material as an equivalent circuit of RC elements.

Figure 4(a) shows the complex impedance plane plots (the Cole–Cole plots) measured at various temperatures. The plots in the complex plane consist of two semicircles with their centres lying below the real axis. This is a result of the distribution of relaxation times, which makes the semicircles depressed from perfect ones in the pure Debye relaxation case. From high frequency to low frequency, two semicircles are attributed to the grain and grain boundary respectively. This is consistent with the results above that the lower-frequency peaks are attributed to the relaxation of the grain boundary layers, while the higher-frequency peaks are attributed to the effects inside the grains.

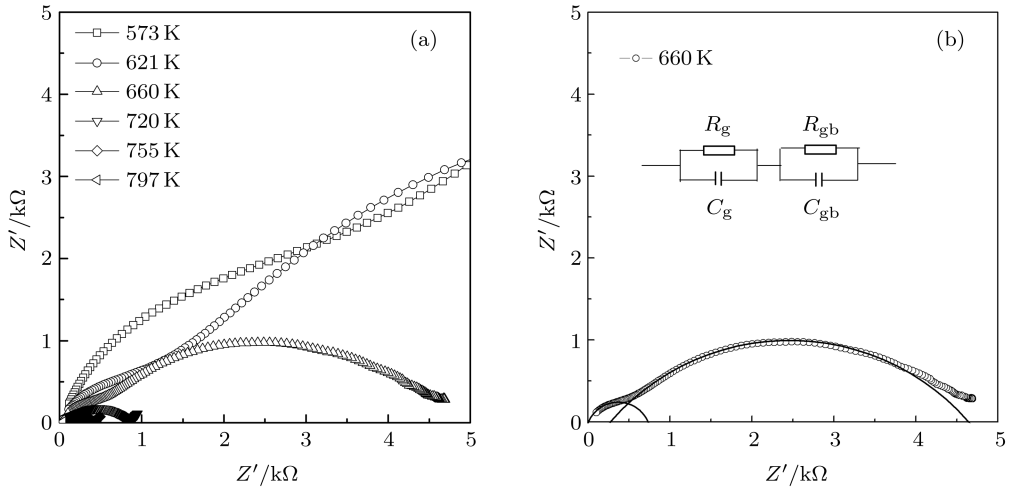


Fig.4. (a)Cole–Cole plots for $Bi_5TiNbWO_{15}$ measured at various temperatures. (b) Equivalent circuit of the Cole–Cole plot for the sample measured at 660 K.

Figure 4(b) shows the Cole–Cole plots of the sample measured at 660 K for clarity. The intercept of the semicircle on the real axis gives the resistance of the corresponding component. The values of the grain resistance (R_g) and the grain boundary resistance (R_{gb}) are calculated to be $R_g = 0.70\,k\Omega$ and $R_{gb} = 4.35\,k\Omega$ respectively. The capacitance (C) can be calculated by using the formula $\omega\tau = 2\pi\, f_{max} RC = 1$, where f_{max} is the frequency of the maximum of semicircles.[15] The values of C_g and C_{gb} are 9.51×10^{-11} and 5.11×10^{-9}F respectively.

Figure 5 illustrates the Arrhenius plots of $\ln\sigma$ versus $1000/T$ for the sample. From the fitting line, it can be seen that the conductivity data obey the Arrhenius law quite well in the temperature range from 550 to 830 K. The values of conductivity activation energy (E_{cond}) for grain itself and grain boundary are about 0.57 eV and 1.11 eV respectively. The conductivities at 625 K for two components are about 1.12×10^{-2} S/m and 1.43×10^{-3} S/m respectively. The

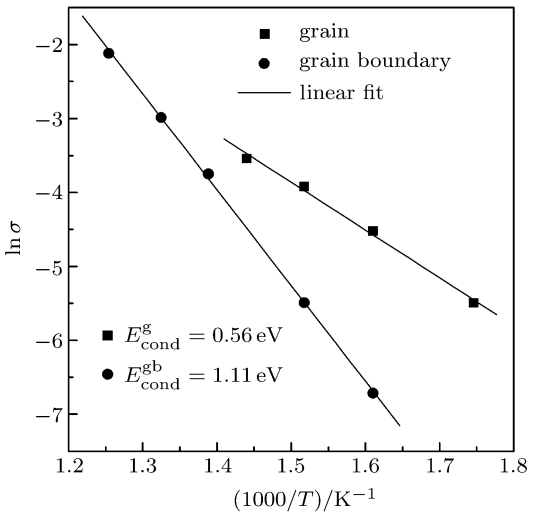


Fig.5. Arrhenius plots of the grain and grain boundary conductivity for $Bi_5TiNbWO_{15}$ ceramic. σ is in unit of Ω·cm.

grain boundary will act as an electric barrier in the polycrystalline ceramic, so the electrical conductivity is higher in the grain than that in the grain boundary.

According to the Schottky barrier model, the grain boundary space charge potential $\Delta\Phi$ is related to the grain boundary and the bulk relaxation times, their ratio is given by[18]

$$\tau_{\mathrm{gb}}/\tau_{\mathrm{g}} = \exp(e\Delta\Phi/k_{\mathrm{B}}T)/(2e\Delta\Phi/k_{\mathrm{B}}T), \qquad (2)$$

where e is the elementary charge, k_{B} and T have their usual meanings. The peak of the semicircle allows us to calculate relaxation time with the relation: $\omega_{\mathrm{p}}\tau_{\mathrm{p}} = 1$. According to this, $\Delta\Phi \approx 0.52\,\mathrm{eV}$ at 660 K is calculated. From the Arrhenius plot above, we can easily find that the value of $E_{\mathrm{cond}}^{\mathrm{gb}} - E_{\mathrm{cond}}^{\mathrm{g}}$ is equal to 0.54 eV, agreeing well with the grain boundary space charge potential $\Delta\Phi$ of 0.52 eV.

From the fitting results above, it is obvious that the activation energies for relaxations and conductivity are different from each other in the selected temperature range. The values of E_{relax} are always slightly higher than E_{cond} obtained from conductivity plots. This character suggests that the relaxation process does not govern the electrical conduction and indicates that the relaxation is a dipolar type. It should be considered that various types of conducting carriers all contribute to the electrical conduction at higher temperature region, although they may be not related to the dielectric relaxation/polarization. For instance, the electrons released from the oxygen vacancy which can be the source of the space charge polarization, are easy to thermally activate and become conducting electrons. Hence, the conductivity energy obtained is lower than the relaxation one. These dipoles related to oxygen vacancies and electrons may be driven to the grain boundaries and would be easily trapped. The grain boundaries thus block the ionic transport across them and then induce the lower electric conductivity than that in the grain. The accumulation of the space charges in the interfaces of the grain boundaries produces the space charge potential $\Delta\Phi$ of 0.52 eV.

4. Conclusions

In summary, the dielectric and conductivity properties of $Bi_5TiNbWO_{15}$ were studied by using dielectric relaxation and AC impedance spectroscopy in detail. Two distinct relaxation mechanisms associated with oxygen vacancy were detected in the frequency of 10 Hz–13 MHz. One mechanism may be attributed to the hopping process of the oxygen vacancies inside the grains, another mechanism seems to be associated with the space charges bound at the grain boundary layers.

References

[1] Kikuchi T 1976 *J. Less-Common Met.* **48** 319
[2] Kikuchi T, Watanabe A and Uchida K 1977 *Mater. Res. Bull.* **12** 299
[3] Mercurio D, Trolliard G, Hamsen T and Mercurio J P 2000 *Int. J. Inorg. Mater.* **2** 397
[4] Luo S, Noguchi Y, Miyayama M and Kudo T 2001 *Mater. Res. Bull.* **36** 531
[5] Noguchi Y, Miyayama M and Kudo T 2000 *Appl. Phys. Lett.* **77** 3639
[6] Zhu J, Chen X B, Lu W P, Mao X Y and Hui R 2003 *Appl. Phys. Lett.* **83** 1818
[7] Zhu J, Lu W P, Liu Q C, Mao X Y, Hui R and Chen X B 2003 *Acta Phys. Sin.* **52** 2627 (in Chinese)
[8] Zhu J, Mao X Y and Chen X B 2004 *Acta Phys. Sin.* **53** 3929 (in Chinese)
[9] Goda K and Kuwabara M 1991 *Ceram. Trans.* **22** 503
[10] Bidault O, Goux P, Kchikech M, Belkaoumi M and Maglione M 1994 *Phys. Rev.* B **49** 7868
[11] Li W, Chen A P, Lu X M and Zhu J S 2005 *J. Appl. Phys.* **98** 024109
[12] Ang C, Yu Z and Cross L E 2000 *Phys. Rev.* B **62** 228
[13] Sinclair D C and West A R 1989 *J. Appl. Phys.* **66** 3850
[14] Srinivas K and James A R 1999 *J. Appl. Phys.* **86** 3885
[15] Sinclair D C and West A R 1994 *J. Mater. Sci.* **29** 6061
[16] Wang Z Y and Chen T G 1998 *Phys. Status Solidi* A **167** R3
[17] Shulman H S, Damjanovic D and Setter N 2000 *J. Am. Ceram. Soc.* **83** 528
[18] Balaya P, Jamnik J, Fleig J and Maier J 2006 *Appl. Phys. Lett.* **88** 062109